

SIMON ALGORITHM IN MEASUREMENT-BASED QUANTUM COMPUTING

M. SCHWETZ and R. M. NOACK

*Fachbereich Physik, Philipps Universität Marburg, Renthof 6
35037 Marburg, Germany*

maximilian.schwetz@physik.uni-marburg.de

Simon's hidden subgroup algorithm was the first quantum algorithm to prove the superiority of quantum computing over classical computing in terms of complexity. Measurement-based quantum computing (MBQC) is a formulation of quantum computing that, while equivalent in terms of computational power, can be advantageous in experiments and in displaying the core mechanics of quantum algorithms. We present a reformulation of the Simon algorithm into the language of MBQC—in detail for two qubits and schematically for n qubits. We utilize the framework of ZX-calculus, a graphical tensor description of quantum states and operators, to translate the circuit description of the algorithm into a form concordant with MBQC. The result for the two-qubit Simon algorithm is a ten-qubit cluster state on which single-qubit measurements suffice to extract the desired information. Additionally, we show that the n -qubit version of the Simon algorithm can be formulated in MBQC as cluster state graph with $2n$ nodes and n^2 edges. This is an example of the MBQC formulation of a quantum algorithm that is exponentially faster than its classical counterpart. As such, this formulation should aid in understanding the core mechanics of such an established algorithm and could serve as a blueprint for experimental implementation.

Keywords: Measurement-based Quantum Computing; ZX-Calculus; Simon algorithm.

1. Introduction

Measurement-based quantum computing (MBQC) is an alternate approach to quantum computing that is conceptually different than the canonically used circuit model.¹ In contrast to the circuit model, in which entangling multi-qubit gates effectuate the computing power of quantum mechanics, MBQC pre-encodes the entanglement in a highly entangled multi-qubit initial state that is prepared in advance. Typically, this resource state is a cluster state, an eigenstate of the ZXZ -stabilizer that is the ground state of lattices with Ising interaction.² Other states, such as the two-dimensional AKLT state with spin greater than $3/2$, are also possible, but the information processing protocol will deviate from the canonical approach to MBQC.^{3,4} Single-qubit measurements on the entangled initial state are then sufficient to implement quantum computing in full generality.^{1,5,6} The MBQC model can lead to alternate experimental implementations of quantum algorithms that can, in some cases, be more flexible and efficient than circuit-based implementations. In addition, it is useful for highlighting and understanding certain fundamen-

tal aspects of quantum computing that are not equally prominent in circuit-based quantum computing.

From an experimental point of view, it is convenient that, in MBQC, the quantum-specific part in the form of entanglement is carried out at the beginning of the process. This preparation of the initial cluster state could be outsourced to a device whose sole purpose is generating entanglement. The prepared state would then be handed over to a device that need only carry out one-qubit measurements. The latter are—in comparison with entangling multi-qubit gates in a circuit-based setup—easy to perform. The composite device would, in effect, function as a universal quantum computer. On a fundamental level, MBQC leads to a compelling alternate picture of quantum computing: one reason for the advantage of quantum computing over classical computing can, among other properties, be found in the necessity to generate a multi-qubit entangled state. Hence, the creation of such a state is generally difficult because it cannot be carried out by any classical device. The measurements carried out in the subsequent phase of MBQC can be interpreted as classical tools that utilize the previously created resource of quantum entanglement for calculational purposes. The pedagogical appeal of this framework is that the “quantumness” and the classical operations are clearly separated. This picture can potentially provide a better understanding of where the advantage over classical computing actually lies.

In other contexts, the circuit model might nevertheless be the more suitable framework to utilize. The set of tools for information processing in the circuit model is analogous to the logic-gate model of classical computing in which elementary logic gates are used as building blocks to compose a complex algorithm. The decomposition into a small set of fundamental elements as well as the resulting linear flow of information processing from left to right in a diagram reminiscent of the canonical model of classical computing. In MBQC, the flow of information processing during a computation is much less evident due to the multi-dimensional architecture of a graph state. In addition, in the quantum circuit model, the actual effect of one gate on a set of qubits can be denoted much more compactly and understandably than its analog in MBQC, the effect of a single-qubit measurement on a highly entangled multi-partite state.

In MBQC, the key element for information processing is a sequence of measurements on the qubits of a cluster state. The measurements are carried out along selected axes to realize a specific algorithm. Models such as the *measurement calculus*⁷ or the *monad*⁸ description have been formulated to try to encompass the complexity of MBQC. In this paper, we will utilize the graphical notation of the *ZX-calculus*, which is able to represent graph states as well as graph-like operators in a unified way.⁹ This graphical calculus was introduced for carrying out derivations in multi-qubit quantum computation and information. On a computational level, the diagrams are tensor-network descriptions of both quantum states and quantum operators; in fact, the notation does not distinguish between the two. The ZX-calculus is also naturally suited to describe cluster states in arbitrary topolo-

gies and has a primitive notation to denote projective, single-qubit measurements. Therefore, it is a framework that is well-suited for describing MBQC in an intuitive manner.

The set of calculation rules that can be applied within ZX-calculus are not only used for transforming ZX-diagrams into one another, but are also capable of translating an algorithm formulated in terms of quantum circuits to the language of MBQC.¹⁰ The aforementioned rules are equations that tell the user how to transform ZX-diagrams. On a low level, they simply represent tensor equations. They range from single-node identities to large-scale node and edge manipulations in the graph of a ZX-diagram. One application for these rules is to simplify diagrams and thus to optimize quantum circuits.¹⁰ Another application of the ZX-calculus is to translate quantum circuits into the language of ZX-diagrams; we will do this here. Subsequently, we will use the rules mentioned above to transform these diagrams into a specific format to reformulate the oracle of the Simon algorithm as a measurement-based quantum calculation. This work directly builds on previous work of the authors in which the three-qubit Deutsch-Jozsa algorithm in MBQC is derived.¹¹

The algorithm proposed by Daniel Simon in 1993 and published in 1994 was the first quantum algorithm that was proven to be exponentially faster than any classical computation on the same problem.¹² The algorithm solves a “promise problem” in which a “black-box” oracle executes a function with a property that is not known initially but is promised to lie within a given set of properties. The specific proposal by Simon was to find the period of a function, that is, the numerical distance between two inputs that trigger the same output. The algorithm was later generalized to solve a general *hidden subgroup* problem on arbitrary groups.^{13,14} Even though Simon did not fully realize the significance of his development immediately, the Simon algorithm subsequently inspired Peter Shor to apply a similar theoretical idea to the problems of factoring and discrete logarithms.¹⁵ Eventually, this led to the development of Shor’s famous algorithm for prime factorization, a lighthouse in the realm of quantum algorithms.¹⁶

Our goal will be to derive a measurement-based formulation of the Simon algorithm in a systematic way using the ZX-calculus. We will start by introducing the Simon algorithm in the canonical language of circuit-based quantum computing in Sec. 2. In a deeper analysis, we will investigate the forms of the possible oracles and will formulate a deterministic algorithm to translate a given periodic function to a circuit for the oracle in Sec. 3. Sec. 4 will serve to reformulate the oracle circuits in terms of MBQC and will use the two-qubit version of the algorithm as an example. The result will be a ZX-diagram that incorporates both the form of the required cluster state as well as a recipe for the single-qubit measurements that realizes the Simon algorithm in MBQC. After having illustrated the concepts and procedure for the two-qubit case, in Sec. 5 we will go on to describe the topology of resource cluster states for n qubits. We will observe that the algorithm gains complexity in the sense of the increase in the number of cross sections within the required graph

state pictured in two dimensions. Finally, in Sec. 6, we will discuss the key aspects of this work and give an outlook for potential future work.

2. Simon algorithm

A function f is said to have a period s if all elements of its domain that are separated by s yield the same image under f . Consider a function $f : \mathbb{S}^n \rightarrow \mathbb{S}^n$, where $\mathbb{S} = \{0, 1\}$, which maps from n -bit binary numbers to n -bit binary numbers. Its period s is defined as

$$\exists! s \in \mathbb{S}^n : \forall a, b \in \mathbb{S}^n, a \neq b : f(a) = f(b) \Leftrightarrow a = b \oplus s, \quad (1)$$

where \oplus is bitwise addition modulo 2. From now on we will use the terms *periodic* and *period* to refer only to a function that fulfills the aforementioned definition of periodicity modulo 2 and not other definitions of periodicity. When $s \neq 0$, the function is *two-to-one*, and when $s = 0$, the function is *bijective*. Given such a periodic function, the aim of the Simon algorithm is to determine the period s of f . We assume that the function is only accessible as a black box (oracle), which can act on a (quantum) input, but that no information about the internal properties of the black box is available.

The Simon algorithm works by applying the function f to an n -qubit quantum state that is a superposition of all possible inputs. The output of f is stored on n auxiliary qubits, and each pair of input basis states that are s apart are “marked” by the same basis state as on the auxiliaries. This scheme generates entanglement that groups together pairs of basis states that are a period s apart. A quantum-interference-based filter subsequently is used to filter out a bit string t that fulfills the linear equation $s \oplus t = 0$. After the procedure is repeated sufficiently many times to obtain a sufficiently large set of linearly independent values of t , a classical solver for systems of linear equations can be used to solve for the period s .

We start with n working qubits, where n is equal to the dimension of the function domain and image, each prepared to be in the state $|+\rangle \simeq |0\rangle + |1\rangle$. (Note that we omit normalization here and throughout this paper.) In addition to the working qubits, we will need n auxiliary qubits, initially prepared to be in the state $|0\rangle$. The full Simon algorithm, including the initial states and the measurement of the final state, is depicted schematically in Fig. 1.

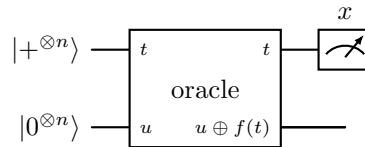


Fig. 1. Simon algorithm in the quantum circuit framework.

We assume that the oracle applies the function f to a register of n working

qubits, putting the result in the register of n auxiliary qubits. In doing so, we additionally assume that the oracle takes into account the output value of the function f and maps a general basis state of the full system (working and auxiliary register) $|t\rangle|x\rangle$ as $|t\rangle|x\rangle \rightarrow |t\rangle|x \oplus f(t)\rangle$. Since all qubits of the auxiliary register are prepared in the $|0\rangle$ -state, the effect of the oracle is to map $|t\rangle|0^n\rangle \rightarrow |t\rangle|f(t)\rangle$, and we end up with the image under f of the working register in the auxiliary register. Thus, after the application of the oracle, the system is in the entangled state

$$|\psi\rangle = \sum_{t \in \{0,1\}^n} |t\rangle |f(t)\rangle. \quad (2)$$

In effect, basis states $|t\rangle$ and $|t'\rangle$ for which $t' = t \oplus s$ in the working register are “marked” by the same basis state of the auxiliary register, $|f(t)\rangle = |f(t')\rangle$.

The final step of the quantum algorithm as depicted in Fig. 1 is the measurement of the qubits of the working register in their respective x -bases; the possible measurement outcomes will lie in $\{+, -\}^n$. However, instead of carrying out the measurements in the x -basis, we could apply an n -qubit Hadamard gate $H^{\oplus n}$ to the working register and then carry out the measurements in the computational z -basis. After the Hadamard gate, the total state in eq. (2) transforms to

$$\begin{aligned} |\psi'\rangle &= \sum_{r \in \{0,1\}^n} \sum_{t \in \{0,1\}^n} (-1)^{r \cdot t} |r\rangle |f(t)\rangle \\ &= \sum_{r \in \{0,1\}^n} \sum_{b \in \text{Im}(f)} \sum_{f(a)=b} (-1)^{r \cdot a} |b\rangle. \end{aligned} \quad (3)$$

If $s = 0^n$, f is a *one-to-one* function, and $|\psi'\rangle$ simplifies to

$$|\psi'_{s=0}\rangle = \sum_{r \in \{0,1\}^n} \sum_{t \in \{0,1\}^n} (-1)^{r \cdot t} |r\rangle. \quad (4)$$

If we now perform a measurement on the working qubits—which are in state (4)—in the computational basis, all measurement outcomes have the same probability. This also holds for the original case in which the n -qubit Hadamard gate is not present, and the measurement is carried out in the x -basis. As $s = 0^n$ in this case, all outcomes m satisfy $s \oplus m = 0$.

For the case of a non-vanishing period $s \neq 0^n$, f is a *two-to-one* function, and eq. (3) can be rewritten as

$$|\psi'\rangle = \sum_{r \in \{0,1\}^n} \sum_{b \in \text{Im}(f)} \left[(-1)^{r \cdot a_1} + (-1)^{r \cdot a_2} \right] |r\rangle |b\rangle, \quad (5)$$

where $f(a_1) = f(a_2) = b$. Using that $a_2 = a_1 \oplus s$, we obtain

$$\begin{aligned} |\psi'\rangle &= \sum_{r \in \{0,1\}^n} \sum_{b \in \text{Im}(f)} \left[(-1)^{r \cdot a_1} + (-1)^{r \cdot a_1 \oplus s} \right] |r\rangle |b\rangle \\ &= \sum_{r \in \{0,1\}^n} \sum_{b \in \text{Im}(f)} \left\{ (-1)^{r \cdot a_1} [1 + (-1)^{r \cdot s}] \right\} |r\rangle |b\rangle. \end{aligned} \quad (6)$$

The term in square brackets in the last line of eq. (6) will vanish if and only if $r \cdot s = 1$ and will be non-zero only when $r \cdot s = 0$. Thus, measuring the working qubits in the computational basis will generate an outcome m that satisfies $m \cdot s = 0$. This result also holds for the circuit without the n -qubit Hadamard gate as long as the measurement is carried out in the x -basis.

After a single measurement of the working qubits, we obtain one binary number m that satisfies $m \cdot s = 0$, but not s itself. In order to determine s , the quantum part of the algorithm must be executed repeatedly until $n - 1$ linearly independent outcomes m are obtained. The resulting set of $n - 1$ linear equations can be solved using a classical algorithm to obtain s , provided that $s \neq 0^n$. If $s = 0^n$, the result is indeterminate, as any m will satisfy $m \cdot s = 0$. To make sure that $s \neq 0^n$, we can simply apply f to two different inputs a_1 and a_2 that satisfy $a_2 = a_1 \oplus s$, where s is the solution of the set of linear equations. If $f(a_1) = f(a_2)$, we know that f is a *two-to-one* function for which we have obtained the correct period s . If, on the other hand, $f(a_1) \neq f(a_2)$, the function f must be *one-to-one* with $s = 0^n$.

3. Oracle

3.1. Oracle design

Up to now, we have conceptualized the oracle as a black box that applies a particular instance f of a class of possible oracle functions to an arbitrary input state consisting of n working qubits and n auxiliary qubits. Mathematically, the operation that is carried out is to add the image under f of the state of the working qubits to the state of the auxiliary qubits, as has already been visualized in Fig. 1. For practical application, however, the oracle must have a physical implementation that depends on and implements a particular specific instance f . We now consider how to carry out such an implementation in a quantum circuit picture with the aim of subsequently reformulating the implementation in MBQC.

Since the function of the oracle is to add bits (modulo 2) to the auxiliary qubits conditionally depending on the state of the working qubits, it is natural to use CNOT gates to construct the circuit implementing f . A CNOT gate will, for a two-qubit basis state, add a bit (modulo 2) to the state of the second qubit if and only if the first qubit is in the state $|1\rangle$. Mathematically, the gate can be written as

$$\text{CNOT} = |00\rangle\langle 00| + |01\rangle\langle 01| + |10\rangle\langle 11| + |11\rangle\langle 10|. \quad (7)$$

Since the oracle can include information flow from all working to all auxiliary qubits, a circuit formulation should also be able to include any CNOT gate that has one of the working qubits as its control and one of the auxiliary qubits as its target.

Normally, the CNOT gate is only activated when the first (control) qubit is 1. However, here it is convenient to be able to activate the CNOT using a 0 as the control condition. We can do this by adding an X gate to the auxiliary qubit. Since the function of an X gate is to swap each bit in the qubit basis, following a CNOT with an X gate implements a control gate in which the bit is flipped in the second

qubit's basis if and only if the basis state of the first qubit is $|0\rangle$. As there is freedom to displace the X gates to the right in the quantum circuit, we group all X gates as the last possible operation of the oracle.

Note that the X gates described above are actually not required for the algorithm. As is evident in Fig. 1, adding single-qubit gates to the auxiliary register does not affect the outcome of the measurement on the working register. Indeed, the essential ingredient for finding the period is the entanglement between working and auxiliary qubits. Nevertheless, a case may be made for retaining the X gates within our theoretical treatment. The primary reason is that we need to check that the found period s is correct in the classical post-quantum processing of the algorithm (e.g., in order to determine if $s = 0$). For a general oracle, the value of f is available in the auxiliary qubits, and we can check any value by sampling. While a reduced oracle without X gates will still be able to tell us if the images of two samples under f are the same, it will not yield the true value of the image under f . In this paper, we retain the X gates, implementing the most general version of the oracle.

A specific set of such gates for one particular instance f of the oracle function is depicted in Fig. 2. Indeed, this instance contains the maximum number of possible gates for oracles in the Simon algorithm. Other instances of f would require fewer gates, that is, some of the gates in Fig. 2 would be present and some absent. Each unique combination from this maximum set of possible gates realizes one particular instance of f .

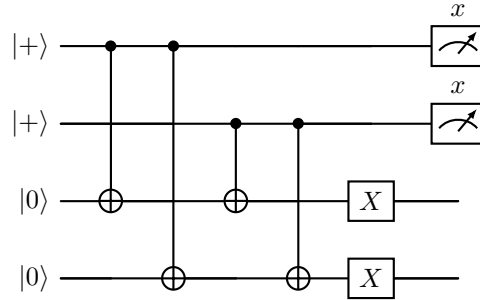


Fig. 2. One particular instance of the 2-qubit oracle for Simon's algorithm along with the the initial states and measurement operations. The oracle instance shown in the figure is the one with the maximum number of gates. Other instances of f imply that some of the shown gates are "switched off".

3.2. Generalization

Now that we have shown that the oracle for any n -bit periodic function f can be realized as a network consisting of CNOT gates between n working and n auxiliary qubits and X gates acting on the auxiliary qubits, we want to reformulate the

network for such an oracle in MBQC. In order to do this, we must first gain a formal understanding of which realization of the function f corresponds to what combination of CNOTs and X gates. In the following, we formulate a deterministic algorithm to construct a quantum network implementing the oracle for a given periodic function f .

A general n -qubit function f has 2^n possible outputs ($|\text{Im } f| = 2^n$). Each output ω_σ is the image of a basis state σ of the domain. For example, $\sigma = 010$ might be a basis state and $\omega_\sigma = 110$ its corresponding image, so $f(010) = 110$. We define the *characteristic* \mathcal{C}_f of the function f as the output string of all computational-domain basis states

$$\mathcal{C}_f = \prod_{\sigma \in \mathbb{Z}_2^n} \text{"}\omega_\sigma\text{"} = \omega_{0\dots 00} \omega_{0\dots 01} \cdots \omega_{1\dots 11}, \quad (8)$$

where the double quotes “...” indicate that the meaning of the product is to concatenate the binary numbers. For n qubits, the characteristic of a function is a string of length $n 2^n$ bits. For example, the two-to-one function g that is defined by

$$g(00) = 10, \quad g(01) = 01, \quad g(10) = 01, \quad g(11) = 10 \quad (9)$$

would be represented by the characteristic

$$\mathcal{C}_g = \underbrace{10}_{g(00)} \underbrace{01}_{g(01)} \underbrace{01}_{g(10)} \underbrace{10}_{g(11)}. \quad (10)$$

Any classical mapping f with period modulo 2 between input and output qubits can be implemented as a quantum network consisting of CNOT gates acting on particular pairs of input and output qubits along with X gates on the output qubits. We will encode a configuration of these gates as a concatenated binary string of length $n 2^n$, as we have done for the characteristic of the function in eq. (8). We define the characteristic of a CNOT gate between input qubit i and output qubit j to have ones at the bit positions at which the corresponding basis vector is changed. Mathematically, we define the characteristic of a CNOT gate as

$$[\mathcal{C}_{\text{CNOT},j,k}]_m = \begin{cases} 1, & m = (2^n - lj - 1)n + k, \quad \forall l \in \mathbb{N}, 0 \leq l < n, \\ 0, & \text{otherwise} \end{cases}, \quad (11)$$

where $(j, k \in \mathbb{N}, 1 \leq j, k \leq n)$. In words, we divide the characteristic into 2^n sets of n bits, with each set corresponding to one input basis state. That is, the first n bits are the image of the first basis state, the subsequent n bits are the image of the second basis state, and so on. A CNOT gate will generate non-zero bits only in the n -bit sets that correspond to basis states for which the tested control bit is 1. Each bit of these n -bit sets corresponds to one of the n output bits, so the first bit of the characteristic is the first output bit of the first input basis state. Within such a set, the bit corresponding to the target qubit is 1, and all others are 0.

As an example, we consider a system with two domain and two image bits. This directly implies that the characteristic of both the function and the gates have a

length of $2 \cdot 2^2 = 8$ bits. Furthermore, we take the CNOT gate to act between qubit 1 of the domain and qubit 2 of the image, as depicted in the circuit of Fig. 3. The characteristic of this gate, according to eq. (11), is

$$[\mathcal{C}_{\text{CNOT},1,2}]_m = \begin{cases} 1, & m \in \{5, 7\} \\ 0, & \text{otherwise} \end{cases} \Rightarrow \mathcal{C}_{\text{CNOT},1,2} = 00000101. \quad (12)$$

This characteristic has the following content: The control qubit is the first qubit. Hence, the third and fourth set of $n = 2$ bits, corresponding to the basis vectors 10 and 11, are not all zero. Within these sets, the second bit is set to 1 because the target qubit of the CNOT gate is the second of the image qubits.

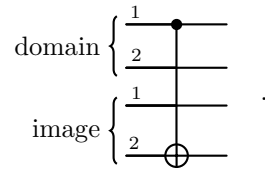


Fig. 3. Circuit for the CNOT gate with control bit 1 and target bit 2 for a 2-bit system.

Analogously to the CNOT gate of eq. (11), we can characterize the X gate on image qubit k as

$$[\mathcal{C}_{X,k}]_m = \begin{cases} 1, & m = ln + k, \forall l \in \mathbb{N}, 0 \leq l < 2^n \\ 0, & \text{otherwise} \end{cases}. \quad (13)$$

Put in words, this means that the k -th bit of each set of n bits is set to 1, corresponding to the k -th image qubit for each domain qubit. For example, an X gate on the second of two image bits would read $\mathcal{C}_{X,2} = 01010101$.

3.3. Factorization

We want to show that an oracle with CNOT- and X -gates can indeed realize any instance f of a periodic (modulo 2) bitwise function. For that, we outline here a deterministic procedure to implement the oracle for every possible function f . To do this, we will add the characteristics of the possible gates to the characteristic of f until the resulting string no longer contains non-zero bits. The steps required will tell us what combination of gates is needed to realize f .

The function f is represented by its characteristic \mathcal{C}_f . We denote the set of gates that can realize the oracle for any periodic function as $S = \{\text{CNOT}_{jk}, X_k\}$, where $1 \leq j, k \leq n$. As an example, the set S for two qubits is displayed in Table 3.3. We need to determine which subset of S will implement a particular realization of f . This is a factorization of \mathcal{C}_f within the set of characterizations $\mathcal{C}[S] = \{\mathcal{C}(s); s \in S\}$ of the set of gates S .

gate	CNOT ₁₁	CNOT ₁₂	CNOT ₂₁	CNOT ₂₂	X ₁	X ₂
char.	00001010	00000101	00100010	00010001	10101010	01010101
angle	α	β	γ	δ	ϕ	η

Table 1. The set $S = \{\text{CNOT}_{jk}, X_k\}$ ($1 \leq j, k \leq n$), along its characterizations, for two qubits.

This factorization can be carried out in a deterministic, algorithmic way. Notice, for example, that in Table 3.3, the first nonzero bit of each element CNOT_{jk} is in a different position. The only operation that will change the first nonzero bit is an X gate acting on the first image qubit. Hence, adding the characteristic of said gate to the characteristic \mathcal{C}_f with a leading 1 (modulo 2) will flip the first bit to zero. Note, however, that it will also change other bits. Thus, we need to step through the bits of \mathcal{C}_f from left to right. Each time a non-zero bit appears, we add the characteristic of the gate with corresponding first non-zero character. After the application of at most $n2^{n-1}$ gates, the bit string will consist of only zeros. The sequence of gates required to do this uniquely determines the circuit that realizes our chosen f .

Example: Consider the two-qubit function f with $f(00), f(01), f(10), f(11) = 10, 11, 11, 10$. As is easily seen, f has a period $s = 11$ and its characteristic is $\mathcal{C}_f = 10111110$. The characteristics of the possible gates can be read off from Table 3.3. Following the procedure outlined above, we obtain

$$\mathcal{C}_f = 10111110 \xrightarrow{X_1} 00010100 \xrightarrow{\text{CNOT}_{22}} 00000101 \xrightarrow{\text{CNOT}_{12}} 00000000. \quad (14)$$

Thus, the oracle for this particular realization of the 2-bit periodic function f is implemented by the gate sequence $\text{CNOT}_{12}\text{CNOT}_{22}X_1$.

4. Measurement-based quantum computing

In the preceding section, we have formulated a general, deterministic algorithm to generate a sequence of gates that realizes a particular instance of the oracle for the Simon algorithm. In doing so, we have described both the function and the gates within the circuit model of quantum computing. Our task now is to switch to the representation of MBQC, which we will do using the framework of the ZX-calculus.⁹ This intuitive and universal graphical calculus was introduced as a tool for carrying out derivations in multi-qubit quantum computation and information. Here we will only give a very brief summary of its relevant features as well as the specific rules that are needed to carry out the transition from the circuit to the MBQC formulation. A somewhat more extensive introduction that is specific to such a reformulation can be found in Ref. 11. For a comprehensive overview that both describes the formalism and illustrates the power of ZX-calculus for a much wider field of applications, we refer the reader to Ref. 17.

4.1. ZX-calculus

The ZX-calculus is a description of quantum states or quantum operations in terms of graphs that link two types of nodes: *Z*-nodes, colored green (or lightly shaded for the visually impaired reader) here, and *X*-nodes, colored red (darkly shaded). On a tensor level, the *X*-nodes are defined as

$$\textcircled{\alpha} = |0 \dots 0\rangle \langle 0 \dots 0| + e^{i\alpha} |1 \dots 1\rangle \langle 1 \dots 1| \quad (15)$$

and the *Z*-nodes as

$$\textcircled{\alpha} = |+\dots+\rangle \langle +\dots+| + e^{i\alpha} |-\dots-\rangle \langle -\dots-| , \quad (16)$$

where $|\pm\rangle = |0\rangle \pm |1\rangle$ (omitting normalization factors). Incoming and outgoing legs represent degrees of freedom, i.e., tensor indices. We note that all ZX-diagrams were typeset with the *zx-calculus* package.¹⁸

Connecting nodes via edges leads to diagrams that represent either quantum states or quantum operators, depending on the configuration of the outgoing edges. As both states and operators are represented as tensors, we will not explicitly distinguish between them; the nature of a diagram should be clear from the context. As a simple example, the eigenstate of the first Pauli matrix *X* can be written as $\textcircled{\alpha} = |+\rangle$, where we omit the relative phase angle α of the node when it is zero.

Calculations are carried out in the ZX-calculus by applying rules to transform diagrams. Rules can be derived by expressing a diagram in tensor notation and transforming, typically simplifying, the tensor contractions. A comprehensive list of rules is given in Ref. 17. A commonly used special simplification is the representation of the Hadamard gate as a single blue dashed line:

$$H = \textcircled{\frac{\pi}{2}} \textcircled{\frac{\pi}{2}} \textcircled{\frac{\pi}{2}} = \text{---} . \quad (17)$$

In this work, we will utilize the following subset of ZX-calculus rules:

$$\textcircled{\alpha} = \textcircled{\alpha} , \quad (18)$$

$$\textcircled{\alpha} \textcircled{\beta} = \textcircled{\alpha+\beta} , \quad (19)$$

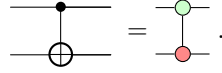
$$\text{---} \textcircled{\alpha} = \text{---} , \quad (20)$$

$$\textcircled{\alpha} = \textcircled{\alpha} . \quad (21)$$

Note that rules (18)-(21) are also valid when *Z*-nodes and *X*-nodes are interchanged in the diagrams. A phenomenological discussion of this set of rules can be found in Ref. 11. All of these properties can be derived canonically within the Hilbert-space model by recognizing that a Hadamard gate is a basis transformation from the *Z*- to the *X*-basis and vice versa.

As stated in the preceding section, we need CNOT gates and *X* gates in order to implement an any particular realization of the oracle of the Simon algorithm.

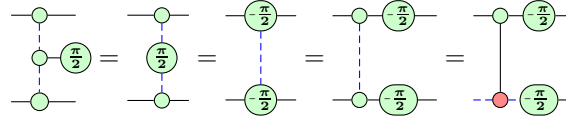
In order to do this in ZX-calculus language, we note that we can write a CNOT operation on two qubits as

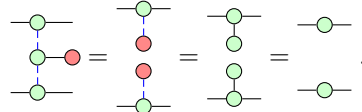

(22)

An X gate can be written in the ZX-calculus simply as a phase- π X -node with one input and one output, i.e.,


(23)

Since a general implementation of the oracle requires the ability to either switch CNOT and X gates on or off, we utilize an adaptive description that can control whether or not these gates appear in the oracle. In particular, we use the adaptive version of a CNOT gate,


(24)


(25)

Eq. (24) tells us that a configuration with a terminal $\pi/2$ -Z-node that is attached to a phase-zero Z-node, which is, in turn, connected to two further Z-nodes via Hadamard-edges is equivalent to the CNOT gate introduced in eq. (11), aside from some phase corrections on the neighborhood. These required correcting phases take on the form of two $\pi/2$ -Z-nodes and two Hadamard nodes and need to be included when this ZX-network fragment is embedded in a larger ZX-diagram. Note that the protruding $\pi/2$ -node in the leftmost part of the equation represents the bra $\langle 0| + i\langle 1|$ and thus acts as a measurement of the unit-eigenvalue eigenstate of the Y -Pauli matrix. We will treat measurements in the scope of the ZX-calculus more thoroughly in the next section.

Eq. (25) shows that inserting a zero-phase X -node rather than $\pi/2$ -Z-node into eq. (24) disconnects the two Z-nodes on the top and on the bottom of the diagram. Thus, one can control whether or not a CNOT gate between two nodes is present by choosing whether there is a $\pi/2$ -Z-node or a zero-phase X -node. Note that the identities (24) and (25) can be derived by applying rules (20)-(21).

4.2. MBQC with the ZX-calculus

For the purposes of this work, the essential feature of a ZX-diagram-based picture is that it provides a natural way to describe measurement-based quantum computing. In order to see why this is, we realize that a ZX-diagram with only Z-nodes

(green) and in which all edges are Hadamard edges (blue-dashed) represents a *cluster state* in which the Z-nodes represent the qubits.¹⁷ A projective measurement with outcome 0 of a qubit along an axis in the x - y -plane can be written as the projector $-\textcircled{\alpha}$, where α is the angle of the basis in the plane. For example, a measurement along the x -axis with outcome 0, corresponding to the projected state $|+\rangle = |0\rangle + |1\rangle$, would be represented by $-\textcircled{0}$. Since all nodes in a cluster state are Z-nodes, one can contract this measurement projection to the associated qubit it is attached to using rule (19). Hence, a ZX-diagram consisting of only Z-nodes and Hadamard edges can also be understood as a sequence of x -measurements on a cluster state. On a technical note, for MBQC within ZX-calculus, it is usually assumed for simplicity that any measurement always has the outcome 0. If the other outcome, 1, were to occur instead, this “error” could be propagated through the network so that either subsequent measurement axes need to be adjusted or the final measurement outcome has to be altered in a manner that directly follows from the phases that occur. We will not elucidate this procedure further here; see Ref. 17 for a detailed explanation.

4.3. Translation to MBQC

In Secs. 4.1 and 4.2, we introduced the prerequisites for characterizing MBQC with the ZX-calculus and described several identities that are required to translate the Simon algorithm to a measurement-based form. Here we will first develop a procedure for the two-qubit algorithm and then explain how it can be expanded to the n -qubit case.

Fig. 2 depicts a schematic circuit for the two-qubit Simon algorithm that includes all gates that could occur in a specific realization of the oracle: CNOT-gates between all pairs of input and auxiliary qubits and X -gates on all auxiliary qubits. Some (or all) of these gates may not be present in a circuit realizing a particular instance of the oracle. Thus, an arbitrary oracle can be constructed by switching on or off particular gates. A general circuit for which each gate can be switched on or switched off can be realized in the ZX-calculus using the adaptive description of the CNOT gate in Eq. (24) and Eq. (25), along with the rules in Eqs. (20)-(21).

A raw translation of the two-qubit circuit is depicted in Fig. 4. Note that we have identified the initial states of the qubits as $|+\rangle = \textcircled{0}$ and $|0\rangle = \textcircled{\pi/2}$. The adaptive CNOT gates are controlled by a node that we depict as

$$\textcircled{\alpha} = \begin{cases} \textcircled{0} & , \quad \alpha = 0 \\ \textcircled{\pi/2} & , \quad \alpha = \pi/2 \end{cases} . \quad (26)$$

This node is adaptive in the sense that it is chosen to be either an X -measurement or a Y -measurement depending on the particular realization of the function that the oracle represents. Which of the two permitted distinct phases, $\alpha = 0$ or $\alpha = \pi/2$, is chosen determines the color of the node. As expressed in eq. (24), the adaptive CNOT gate also requires some extra correcting phases to be applied to

the two qubits adjacent to the one being measured. Those are included into the raw translation by

$$\alpha_c = \begin{cases} 0 & \alpha = 0 \\ \frac{\pi}{2} & \alpha = \frac{\pi}{2} \end{cases}, \quad (27)$$

where α is the same value as in eq. (26). The same scheme applies to all adaptive angles. The nodes in Fig. 4 with angles η and ϕ represent the X gates; the phase of η or ϕ is π if an X gate is present and 0 if not.

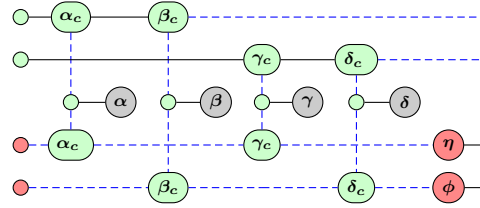


Fig. 4. Raw translation of the two-qubit Simon algorithm into a ZX-diagram.

Starting from the raw translation of Fig. 4, we rewrite and transform the graph into a form consistent with MBQC using the rules presented in Eqs. (20)-(21), yielding Fig. 5. A detailed description of all individual steps taken is given in the appendix to this work; here we give an overview and describe the most important steps.

First, notice that the two protruding edges on the bottom in Fig. 4 represent the auxiliary qubits. Their final state is irrelevant because only the first two (working) qubits are measured. In fact, anything that is done to these branches of the diagram is irrelevant; we can simply omit the bottom legs to simplify the diagram.

A series of relatively straightforward applications of the rules of ZX-diagrams then leads to the diagram depicted in Fig. 5, which implements the two-qubit Simon algorithm in the framework of MBQC. As is required for MBQC, it can be seen that all qubits of the many-body system are Z -nodes. Measurements on these qubits are always carried out in the y - z -plane, at an angle that depends on the corrective factors. The four remaining qubits will be measured in the adaptive manner described above. They are depicted as grey nodes, which either represent a $\pi/2$ - z -measurement or a zero-phase x -measurement.

To clarify the meaning of the MBQC protocol in terms of the ZX-calculus, we give here a short explanation of how to interpret Fig. 5. First, a cluster state, consisting of qubits ordered in a graph as the green nodes connected by blue and dashed lines, is created. Then, all qubits of the cluster state except for the two green nodes to the right are measured according to the angles depicted in the figure. If outcomes other than 0 occur during a measurement, corrective factors must be propagated through the graph; subsequent measurement angles and/or the final result might have to be adapted. Eventually, the two qubits on the right

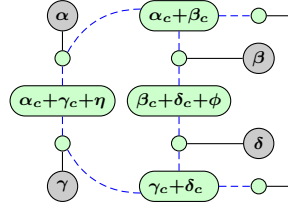


Fig. 5. Measurement-based form of the 2-qubit Simon algorithm.

are measured in the x -basis. For an oracle representing a periodic function, the bit string m that is measured satisfies the condition $m \cdot s = 0$, where s is the period. Finally, it is necessary to repeat the computation sufficiently often to obtain n linearly independent equations for s (where $n = 2$ here), and these equations must be solved classically, just as in the quantum-circuit formulation of the algorithm.

5. n -qubit Simon algorithm

In Sec. 4.3, we derived the MBQC formulation of the two-qubit Simon algorithm. Here we will expand this formulation to treat n qubits. The translation scheme and the following measurement procedure is essentially the same as in the two-qubit case. In the following, we will construct the graphs of the cluster states that are required to formulate the n -qubit Simon algorithm in terms of MBQC.

In the preceding section, we have learned that a general instance of the oracle of the Simon algorithm can be constructed using a network consisting of CNOT gates between arbitrary unique pairs of working and auxiliary qubits. In total, there are n^2 possible CNOT gates, each of which can be realized by an adaptive CNOT gate in the ZX-language. In the ZX-scheme, each pair of working and auxiliary qubits can be pulled together to form one node in the ZX-diagram, so that we obtain n^2 adaptive CNOT gates connecting these nodes. In the two-qubit case, depicted in Fig. 5, we have four qubits, connected by $2^2 = 4$ adaptive CNOT gates. Each node is connected to exactly n other gates.

In order to better display the topology of the graphs of n -qubit, measurement-based oracles, we introduce a compact notation for an adaptive CNOT gate. We define red and dashed lines as

$$- \equiv - \text{---} \text{---} \text{---} , \quad (28)$$

where the dot in the grey node represents the measurement defined in eq. (26) in which the choice of measurement angle determines the presence or absence of a CNOT gate. Since we do not specify the measurement angle explicitly in this notation, we also omit the corrective angles by writing

$$\text{Diagram with a green rounded rectangle containing } \alpha_c + \beta_b + \dots = \text{Diagram with a green circle containing } \cdot, \quad (29)$$

where the corrective angles to be applied to the qubits neighboring the measured node are specified by eq. (27).

The form of the graph for the cluster state of the n -qubit version of the Simon algorithm is determined by the number n of working and auxiliary qubits as well as their connections through adaptive CNOT gates. For visualization, we arrange all qubits on a ring, alternating between auxiliary and working qubits. We then connect each working qubit with all auxiliary qubits via red and dashed lines, which represent adaptive CNOT gates. The working qubits are distinguished by protruding legs that are used for the final measurement. Thus, the n -qubit algorithm is represented by a ring-like graph consisting of $2n$ nodes, n^2 edges, and n protruding legs.

As an example, recall the pattern of the oracle for the two-qubit algorithm, Fig. 5. We place the four qubits (2 working and 2 auxiliary) on a ring, forming a square. Connecting working to auxiliary qubits and introducing protruding legs leads to the schematic diagram depicted in Fig. 6(a). The scheme is easily extended to three qubits, Fig. 6(b), and four qubits, Fig. 6(c).

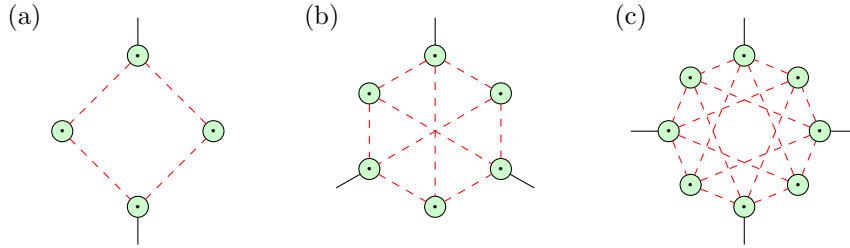


Fig. 6. Topology of the cluster state required to carry out the (a) two-, (b) three- and (c) four-qubit Simon-algorithm in MBQC.

6. Summary and Discussion

In this work, we have reformulated the oracles of the Simon period-finding algorithm in the framework of MBQC, translating quantum-circuit descriptions to ZX-diagrams and then bringing the ZX-diagrams into a form that represents a measurement-based algorithm on a cluster state. An essential intermediate step is the construction of a deterministic algorithm to represent any given periodic function as a quantum circuit consisting only of CNOT and X gates. We have constructed such a MBQC-suited ZX-network explicitly for the two-qubit Simon algorithm; the resulting cluster state consists of eight qubits ordered in the shape of a square. Furthermore, we have described how to construct cluster states for the general n -qubit algorithm and have given explicit forms for such states in the three- and four-qubit cases.

The deterministic algorithm to transform any periodic function into a circuit representation using CNOT and X gates that we have developed in Sec. 2 is an essential part of the procedure to reformulate the Simon algorithm in MBQC. We

know of no such constructive quantum-circuit-based algorithm in the literature. Algorithms to construct an oracle for the Simon algorithm, such as that formulated in Ref. 19, do exist. However, in our understanding, they are all based on the assumption that a specific fixed period s is given. In our opinion, assuming a given period in order to construct an oracle is somewhat circular because the whole purpose of the calculation is to determine an unknown period. In our algorithm, such an assumption would strongly limit the allowed inputs and outputs of the function. It can be argued that such a restriction also, essentially, contains knowledge of the period. Finding the period of a function with no prior knowledge is, in our opinion, the point of applying the Simon algorithm. We remark, however, that guessing the period and subsequently constructing the algorithm around it will become exponentially difficult as the function become larger. We appreciate that the question of how to design oracles for oracular quantum algorithms and, in particular, the issue of how much presupposed knowledge about the function or oracle is available, is still a subject of discussion and, at this point in time, is a somewhat philosophical issue.

Specific quantum circuits for the oracle of the two-qubit Simon algorithm have been published in Ref. 20, albeit without specifying a rigorous algorithm to construct them. We comment that the two-qubit case is of sufficiently low complexity that a working, and presumably optimal, MBQC implementation can be found relatively easily by educated guessing; in our opinion, this is no longer possible for larger systems. Our approach of deterministically constructing implementations of a general oracle for a given algorithm is in line with other published work such as Ref. 21, in which arbitrary oracle circuits are constructed for the four-qubit Deutsch-Jozsa algorithm.

The topology of the cluster states that we have constructed to implement a general n -qubit Simon algorithm gives information about the complexity of the algorithm. We have shown that our graph for the general algorithm consists of $2n$ nodes connected by n^2 edges. Each of these generalized edges consists of one measurement node and two basic cluster-state edges. Thus, as expected, the quantum resources required for the algorithm grow only polynomially with the size of the problem. On the other hand, only the two-qubit Simon algorithm can be realized as a planar (two-dimensional) cluster state. For all larger variants, the graphs do have two-dimensional cross sections, but require a higher number of dimensions for their implementation.

This topological complexity is especially relevant for experimental implementation. A simplified version of the two-bit Simon algorithm has already been experimentally implemented by the authors of Ref. 20. For larger systems, it will be a challenge to implement the cluster states that we have derived. Large quantum states on arbitrary graphs are especially difficult to produce and control, both in solid-state and in photonic systems. We have shown that the number of two-dimensional cross sections increases as the number of bits in the oracle function increase. The increased interconnectivity between qubits will also make the cre-

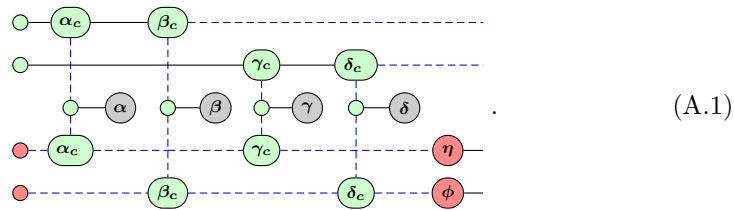
ation of the associated cluster states less tractable.

In this work, we have shown that the MBQC graphs for the oracles are equivalent to their counterparts in the framework of circuit quantum computing. However, we have neither argued nor proven that these are the cluster states that require the smallest number of qubits and/or the smallest interconnectivity. To do this raises a question of optimal minimization that cannot be answered through the framework of ZX-calculus alone because ZX-calculus is only a descriptive language. Nevertheless, the rules of ZX-calculus are a good tool to visualize a path to a minimal solution, as is discussed in Ref. 10. Thus, interesting subjects for future work would be to investigate if the patterns derived here do, in fact, yield a minimal cluster state and, in addition, to formulate schemes for finding such patterns in general and for proving that they are, in fact, minimal.

Historically, Simon's formulation of the Simon algorithm led to Shor's development of his famous prime-factorization algorithm.^{12,15,16} This development sequence can be taken as inspiration for the development of the MBQC-variants of these algorithms. Since the underlying structure of the hidden subgroup problem in the Simon algorithm is also an integral part of the Shor algorithm, it seems only natural to apply the principles of this work to the Shor algorithm. The methods developed here might additionally be useful for reformulating other algorithms, information protocols, error correction codes, etc. in a MBQC picture.

Appendix. Simplification of the oracle in the ZX-language

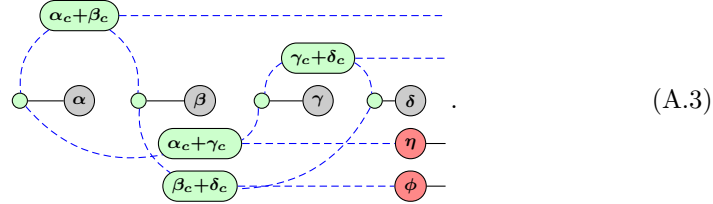
In this appendix, we describe the detailed steps used to reformulate the raw ZX-translation of the two-qubit Simon algorithm as a ZX-network suited for MBQC. For readability, we replicate here the raw translation of the Simon algorithm in Fig. 4,



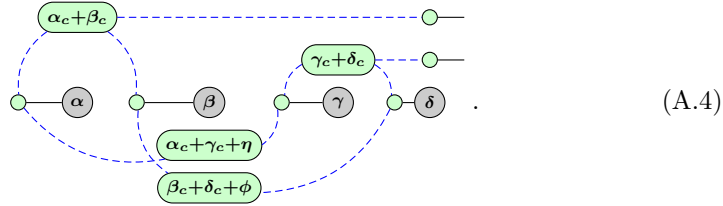
We apply the identities

$$\begin{array}{c} \text{red circle } \alpha \\ \text{with two external lines} \end{array} = \begin{array}{c} \text{green circle } \alpha \\ \text{with two external lines} \end{array} \quad \text{and} \quad \begin{array}{c} \text{green circle } \alpha \\ \text{green circle } \beta \\ \text{with two external lines} \end{array} = \begin{array}{c} \text{green oval } \alpha + \beta \\ \text{with two external lines} \end{array}, \quad (\text{A.2})$$

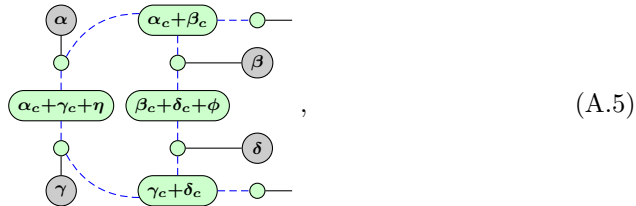
which are rules (18) and (19) in the main text, to obtain an initial simplified version of the oracle,



Since we no longer utilize the information encoded in the auxiliary qubit after applying the oracle, we can omit the protruding legs to the right of the red nodes. More formally, we add a projective measurement $\text{---}\bullet$ in the x -basis to annihilate the protruding legs. Using rules (A.2), we can contract the legs into the neighboring Z-nodes. On the two top-most protruding legs, we then apply the identity $\text{---}\bigcirc\text{---}$ so that they become regular rather than Hadamard legs. Hence, we obtain



A straightforward reordering of the graph yields the result



which we also depict in the main text as Fig. 5 for readability.

References

1. T.-C. Wei, Measurement-based quantum computation (2021).
2. H. J. Briegel and R. Raussendorf, *Phys. Rev. Lett.* **86** (2001) 910–913.
3. T.-C. Wei *et al.*, *Phys. Rev. A* **86** (2012) 032328.
4. A. Miyake, *Annals of Physics* **326** (2011) 1656–1671.
5. R. Raussendorf and H. J. Briegel, *Phys. Rev. Lett.* **86** (2001) 5188–5191.
6. M. A. Nielsen, *Reports on Mathematical Physics* **57** (2006) 147–161.
7. V. Danos *et al.*, *Journal of the Association for Computing Machinery* **54** (2007) 8–es.
8. L. Voufo, *Electronic Notes in Theoretical Computer Science* **270** (2011) 191–210.
9. B. Coecke and R. Duncan, *New Journal of Physics* **13** (2011) 043016.
10. R. Duncan *et al.*, *Quantum* **4** (2020) 279.
11. M. Schwetz and R. M. Noack, [arXiv:2306.13372](https://arxiv.org/abs/2306.13372) (2023).
12. D. Simon, in *Proceedings 35th Annual Symposium on Foundations of Computer Science* (1994) pp. 116–123.

20 *Schwetz and Noack*

13. G. Alagic *et al.*, in *ACM-SIAM Symposium on Discrete Algorithms* (2006) .
14. G. Alagic *et al.*, *ACM Trans. Algorithms* **6**.
15. G. Salton *et al.*, Exploring simon’s algorithm with daniel simon.
16. P. W. Shor, *SIAM Journal on Computing* **26** (1997) 1484–1509.
17. M. Backens *et al.*, *Quantum* **5** (2021) 421.
18. L. Colisson, zx-calculus – a library to typeset zx calculus diagrams.
19. V. authors, Qiskit textbook (2023).
20. M. S. Tame *et al.*, *Phys. Rev. Lett.* **113** (2014) 200501.
21. N. Schuch and J. Siewert, *physica status solidi (b)* **233**.